

Monochrome hybrid, multilevel, halftone screen with unequal spatial resolution for a low-cost electrophotographic printer

Wan-Eih Huang^a, Tongyang Liu^a, Kurt Bengtson^b, Jan Allebach^a

^aSchool of Electrical and Computer Engineering, Purdue University, West Lafayette, IN 47906, U.S.A.

^bHP Inc., Boise, ID 83714, U.S.A.

Abstract

The hybrid screen leverages two halftoning techniques, screening and direct binary search (DBS), to achieve the better quality of the halftoned images, and to enable the algorithm to be integrated into low-cost printers with limited computational resources. This work proposes a complete hybrid screen design method for multilevel output with unequal resolution printing pixels in a laser electrophotographic system.¹ Because of the unstable rendering output of the electrophotographic process, we adopt a clustered-dot screen in our work. We also use the supercell approach to solve the trade-off between screen frequency and the effective number of quantization levels that is inherent to a cluster-dot screen. Moreover, we use subpixel modeling to simulate the unequal resolution printing pixels and multilevel output. This method is well-suited to development of halftoning algorithms for systems with unequal resolution. We also explore several design rules to evaluate the impact on printing quality.

1. Introduction

Monochrome halftoning is a technique for rendering a continuous tone image into an image with binary or a few levels of gray on each pixel.

There are plenty of halftoning algorithms that have been well developed. In general, we can categorize the halftoning algorithms into three basic architectures. First, it is point-to-point processing such as screening or dithering [1] [2]. Second, neighborhood processing, the representative method is error diffusion [3]. The last is search-based algorithms, and usually they are iterative. For example, direct binary search (DBS) [4]. Even though the iterative search based algorithms provide the best quality among these three types of architecture, they need mass computations. Thus, it is impossible to generate halftoned images in real time by iterative search based algorithms. In contrast, screening and error diffusion are widely used in practical implementations due to less computational complexity. However, the iterative search based method is still a crucial tool for designing efficient halftoning algorithms offline. In this paper, we adopt the hybrid screen method [5]. We design the screening algorithm offline by DBS to achieve better quality. Then the halftoned image can be generated in real time by the screening method. As a result, the algorithm is capable to be integrated into a low-cost printer with limited computational resources.

We can classify screens based on the textures they generate. One is cluster-dot screen, clustered individual printer addressable dots form a grid-like pattern. And it produces gray levels by

varying the clustered dots size. In contrast, disperse-dot screen does not form clusters. A number of gray levels are generated by varying the density (frequency) of dots. Clustered dots are more stable than single isolated dots and produce less dot gain as a fraction of area coverage [5]. For our target, laser printer based on electrophotographic process, which has the nature of unstable rendering output, it is more robust to use cluster-dot screen. Nevertheless, there is a trade-off on the design of a cluster-dot screen. The frequency of the clustered dots is referred to as the screen frequency. The screen renders the image detail better with higher screen frequency. The screen renders the image detail better with higher screen frequency. On the other hand, smaller size of screen (higher screen frequency) results in fewer gray levels. Moreover, considering the implementation on a digital printer, the screen frequency must be lower than the printer resolution [5] in order to form clusters. To solve the trade-off between screen frequency and effective number of gray levels, a supercell approach has been proposed [6].

For equal resolution, a printer addressable pixel has the same size in both horizontal and vertical direction. Thus, we can apply the DBS or screening algorithms directly. Because the digital image pixels match the printer addressable pixels. However, for unequal resolution, the printer addressable pixel has different dimension in two directions as illustrated in Fig. 1. Therefore, we use the digital image pixel with identical dimension as a subpixel and then several subpixels grouped with different numbers horizontally and vertically form a simulated unequal resolution printer addressable pixel. In the halftoning algorithm, the subpixels within the same simulated printer pixel have the same binary condition to get close to the real printing output. We will discuss more details in later section.

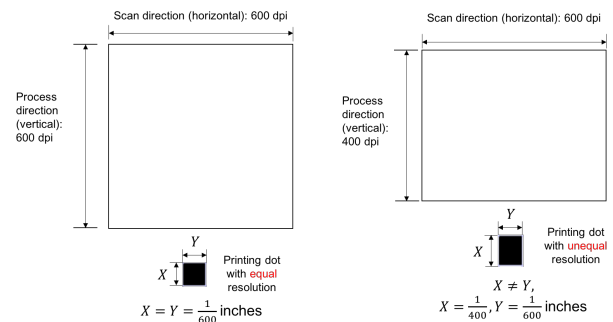


Figure 1: Comparison of equal resolution and unequal resolution. For 600 × 600 dpi, both height and width of a printing dot is $\frac{1}{600}$; For 400 × 600 dpi, height of a printing dot is $\frac{1}{400}$ and width of a printing dot is $\frac{1}{600}$.

¹Research supported by HP Inc., Boise, ID 83714

2. Methodology

Screen Tile Vectors

A periodic screen can be related to two vectors $z = [z_i, z_j]$ and $w = [w_i, w_j]$ defined as screen tile vectors. In order to cover the whole spatial domain with these two vectors, they must be linearly independent. The screen angle is defined as the angle between the tile vector and j-axis in [5]. We can obtain screen tile vectors from the desired lines per inch (lpi) and the process is described in [5]. Our case is unequal spatial resolution. Assume the height and width of each printing dot are X and Y respectively. Then we can obtain the screen tile vectors from the relationship described in Eq. (1), where $R_{gcd} = gcd(\frac{1}{X}, \frac{1}{Y})$ and gcd is the greatest common divisor.

$$\text{screen frequency } \left(\frac{\text{lines}}{\text{inch}}\right) v = \frac{R_{gcd}}{\|XR_{gcd}|w_i|, YR_{gcd}|w_j|\|} \quad (1)$$

Microcell and Supercell

Two screen tile vectors construct a parallelogram called continuous parameter halftone cell (CPHC), and then we can compute the overlapping area of CPHC and 2-D discrete-parameter space to design the microcell [7]. The number of pixels N in a microcell is equal to $|\det [z^T w^T]|$. Fig. 2a shows the microcell obtained by the tile vectors $z = [2, 3]$ and $w = [2, -3]$; and it contains 12 pixels in a microcell. For the purpose of simplifying implementation, the smallest rectangle that can be tiled in horizontal and vertical direction called basic screen block (BSB) is a unit used for storing the screen in a 2-D array [5]. Therefore, the height of BSB is $\frac{N}{gcd(z_j, w_j)}$ and the width of BSB is $\frac{N}{gcd(z_i, w_i)}$ [8]. An example of BSB shown in Fig. 2b which is the corresponding BSB of Fig. 2a.

Supercell obtained by tiling the BSBs in 2-D space is the screen we use for thresholding the continuous tone image. Fig. 3a is an example of a supercell which has 2 BSBs both in horizontal and vertical direction. The height and width of a supercell can be arbitrary integers. However, in practical implementation, we need to consider the cost and the quality. If the screen size is bigger, more memory it needs. If the screen size is smaller, the periodic patterns might be more obvious.

Once the supercell is set, the next step is to design the highlight core and shadow core regions for the stochastic dot texture [2]. That is, the microcell growth sequence of each core might not be the same so that it provides spatial freedom in the halftoned patterns. The core shape is determined by different situations. For example, the square core is suitable for conventional round dot-cluster pattern [2]. In our project, we want to achieve the S shape structure in the midtone, thus we design S shape cores illustrated in Fig. 3b.

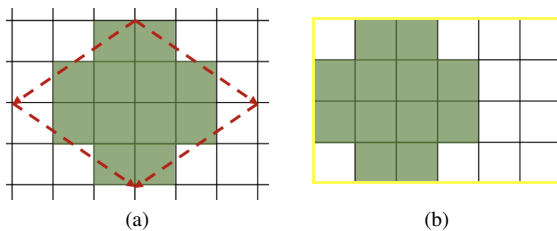


Figure 2: (a) Microcell. (b) BSB.

Screen Generation

The screen generation process can be divided into 3 phases: highlight, midtone, and shadow. In the beginning, we start with an initial random level for which half of the highlight cores have one dot.

Phase 1: To determine the halftoned pattern for the initial gray level, we use *constrained DBS swap*. The candidates of swap pixel can be neighboring pixels within the same highlight core or the pixels in the highlight cores without dots for each trial swap. The trial swap change is allowed only if it minimizes ΔE , the change in visually weighted total squared error, as described later in this paper. After obtaining the halftoned pattern of initial level, we remove dots sequentially based on the halftoned pattern generated in the previous step until no dot remains in the halftone pattern. Similarly, we add dots sequentially based on the halftoned pattern generated in the previous step until all highlight cores contain one dot. How to select a dot to remove or add is using *constrained DBS toggle*. The trial toggle (on or off) change is allowed only if it minimizes ΔE . In this stage, the design of the macrocell index array is completed. Then we can apply this macrocell index array to the remaining microcells levels along with the design constraints within the microcell to generate the halftoned patterns sequentially until all highlight cores are filled. The reason of using the same macrocell index array is reducing the effort of optimization. It is reasonable that if the macrocell sequence achieved good quality in the lower gray levels (lighter) then the higher gray levels (darker) should be also good with the same macrocell sequence, because the effect of the macrocell sequence is more significant in lighter region. Figure 4 illustrates the design process of Phase 1.

Phase 2: Midtone levels are generated by the same macrocell index array obtained in Phase 1 and the microcell dot growing sequence.

Phase 3: A mirroring method is used in the shadow levels. To put it another way, we invert the dot profile function of the highlight core and offset them for the shadow levels.

Unequal Resolution Printing Model

In order to simulate unequal spatial resolution and multilevel output fairly, we adopt subpixels modeling. A square subpixel in the digital image represents part of an ideal printer addressable dot. Hence, we can repeat this kind of subpixel in both the horizontal and vertical directions to form a simulated unequal resolution printer addressable dot.

Take the specification of our implementation as an example, the printer resolution is 600 dpi in the horizontal direction and 400 dpi in the vertical direction, thus the simulated unequal reso-

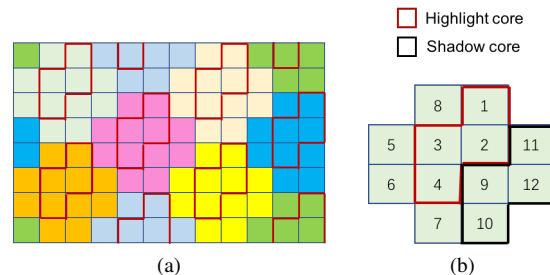


Figure 3: (a) 8×12 Supercell. (b) A microcell with S shape cores.

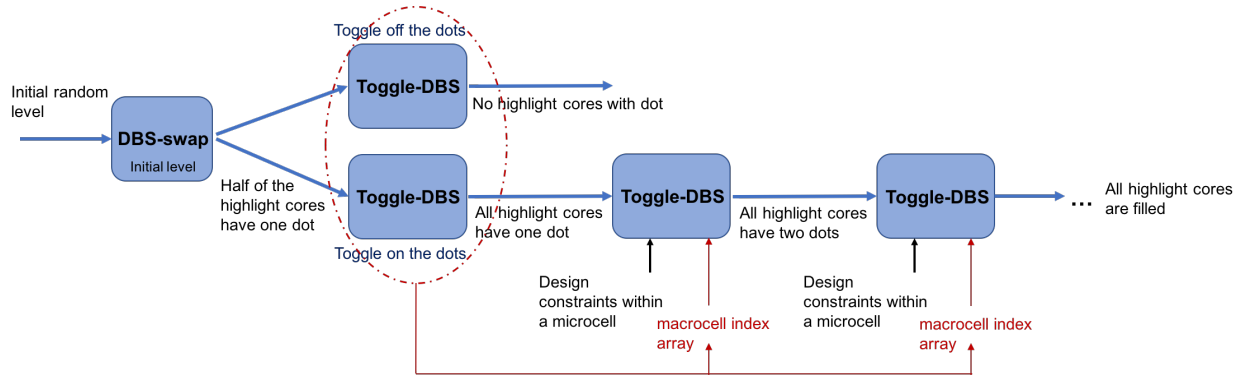


Figure 4: Design process of Phase 1.

lution printing pixel is composed of 3×2 subpixels. Furthermore, considering multilevel output. It is common for laser electrophotographic printers to support multilevel output by PWM (pulse width modulation). In our case, 2 bpp (bits per pixel), a pixel is divided into 3 slivers. Thus, the simulated unequal resolution printing pixel for 2 bpp output is composed of 9×6 subpixels. In addition, each group of 9×2 subpixels in one sliver turns on or off simultaneously. Figure 5 shows the subpixels model we use in this project.

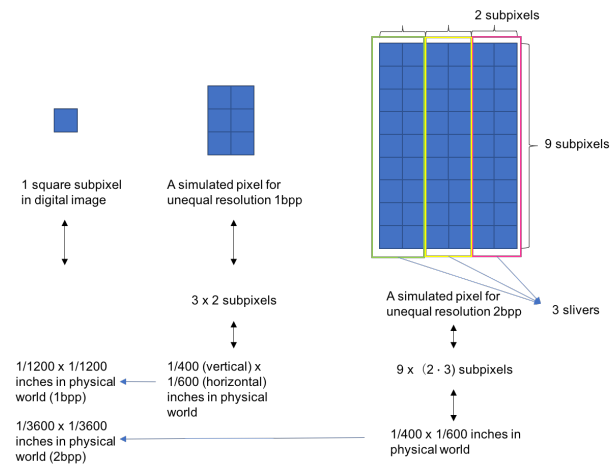


Figure 5: Subpixels modeling.

DBS for unequal resolution

DBS for multilevel applications [9] and DBS for multiple pixels changes [10] have been proposed. Therefore, we can further extend the concept to the unequal resolution DBS. That is to say, DBS on unequal resolution pixel with $\frac{1}{X} \times \frac{1}{Y}$ dpi can be viewed as DBS on several equal resolution subpixels with $\frac{1}{Z} \times \frac{1}{Z}$ dpi which form a simulated unequal resolution pixel. $\frac{1}{Z}$ is the smallest common multiple of $\frac{1}{X}$ and $\frac{1}{Y}$. On DBS swap or toggle operations, all the subpixels within the same unequal resolution simulated pixel switch to the same binary condition due to the fact that they represent a single unit. Hence, the DBS equations can be rewritten. Assume that there are $m \times n$ subpixels within a simulated pixel. And DBS toggle on pixel \mathbf{m}_0 or swap \mathbf{m}_0 and \mathbf{m}_1 . We denote \mathbf{m}_{0ij} as subpixels of \mathbf{m}_0 and \mathbf{m}_{1kl} as subpixels of

\mathbf{m}_1 , where $i \in \{0, 1, \dots, m-1\}$ and $j \in \{0, 1, \dots, n-1\}$. The trial halftone image can be represented by Eq. (2). If the operation is toggle, $a_0 = 1$ and $a_1 = 0$. Otherwise, $a_1 = -a_0$ in swap operation. The change in error due to the trial toggle or swap is given by Eq. (3). Equations (2) and (4) indicate the changes that need to be made should a trial toggle or swap be accepted.

$$g'[\mathbf{m}] = g[\mathbf{m}] + a_0 \sum_{i=0}^{m-1} \sum_{j=0}^{n-1} \delta[\mathbf{m} - \mathbf{m}_{0ij}] + a_1 \sum_{k=0}^{m-1} \sum_{l=0}^{n-1} \delta[\mathbf{m} - \mathbf{m}_{1kl}] \quad (2)$$

$$\Delta E = 2a_0 \sum_{i=0}^{m-1} \sum_{j=0}^{n-1} c_{\bar{p}\bar{e}}[\mathbf{m}_{0ij}] + 2a_1 \sum_{k=0}^{m-1} \sum_{l=0}^{n-1} c_{\bar{p}\bar{e}}[\mathbf{m}_{1kl}] + a_0 a_1 \sum_{i=0}^{m-1} \sum_{j=0}^{n-1} \sum_{k=0}^{m-1} \sum_{l=0}^{n-1} c_{\bar{p}\bar{p}}[\mathbf{m}_{0ij} - \mathbf{m}_{1kl}] \quad (3)$$

$$c'_{\bar{p}\bar{e}}[\mathbf{m}] = c_{\bar{p}\bar{e}}[\mathbf{m}] + a_0 \sum_{i=0}^{m-1} \sum_{j=0}^{n-1} c_{\bar{p}\bar{p}}[\mathbf{m} - \mathbf{m}_{0ij}] + a_1 \sum_{k=0}^{m-1} \sum_{l=0}^{n-1} c_{\bar{p}\bar{p}}[\mathbf{m} - \mathbf{m}_{1kl}] \quad (4)$$

3. Experimental Results

This section shows the experimental results for applying our hybrid screen design with multilevel and unequal spatial resolution output.

In our designs, we apply the compact rule. That is, the newly added sliver should be adjacent to a previous one. In Fig. 6, two halftoned patterns corresponding to the same gray level show an example of the impact of the compact rule. The left image was generated without the compact rule. It means that DBS is free to choose any sliver within the highlight cores. On the other hand, the newly added sliver has to be chosen from the slivers adjacent to the existing slivers in right image generated with the compact constraint. From our result, we can see the objectionable diagonal structure in the left image. And the compact rule reduces these artifacts significantly.

We also consider the centroid (symmetric) rule in our design. In other words, the shift of the centroid of the cluster-dots due to the addition of a sliver must be as small as possible. Figure 7 shows the impact of the centroid rule for two halftoned patterns

with the same gray level. The left halftoned pattern is generated without the centroid rule so there is an objectionable diagonal structure. The right one is generated with the centroid rule and looks more smooth than the left one. Figure 8 is the version of Fig. 7 after applying a Gaussian filter. These images closer to the perception through human eyes.

Figures 9 and 10 show halftoned ramp images thresholding by the screens generated by our approach. The screen Fig. 9 used is a square core design and the screen Fig. 10 used is a S shape core design. Both show good quality.

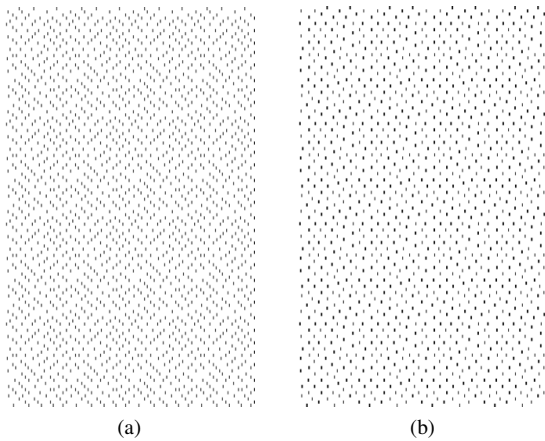


Figure 6: Comparison of the halftoned patterns. (a) The halftoned pattern without compact rule. (b) The halftoned pattern with compact rule.

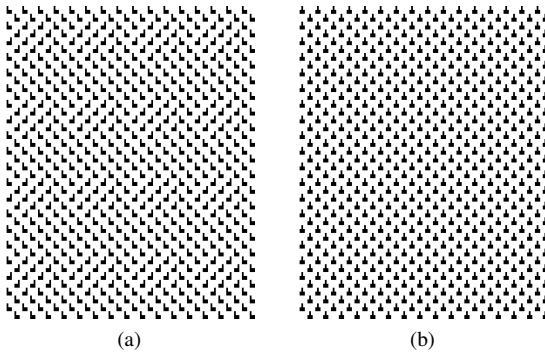


Figure 7: Comparison of the halftoned patterns. (a) The halftoned pattern without centroid rule. (b) The halftoned pattern with centroid rule.

4. Conclusion

In this paper, we developed a novel and complete hybrid screen design method with subpixels modeling. Moreover, we also implemented several version of halftone screens by our approach and they all show good visual results in a real printer. Hence, our method is robust for developing halftoning algorithms for printing systems with unequal spatial resolution.

Acknowledgments

The authors wish to thank Xujie Zhang for providing the Matlab code to generate the ramp image, and for his help to understand the hybrid screening concept.

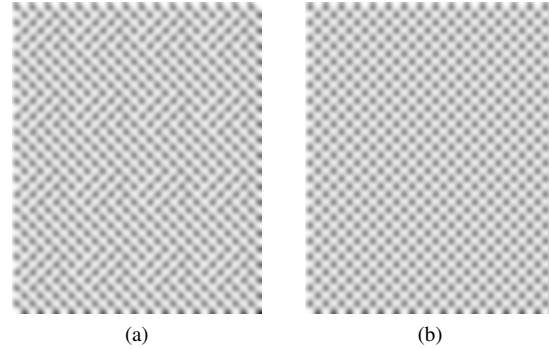


Figure 8: Comparison of the Gaussian filtered halftoned patterns shown in Fig. 7. The standard deviation of the Gaussian filter was $\sigma = 6$ pixels. (a) The halftoned pattern without centroid rule. (b) The halftoned pattern with centroid rule.

References

- [1] Q. Lin and J. P. Allebach, "Color FM screen design using DBS algorithm," in Proc. SPIE, Color Imaging: Device-Independent Color, Color Hardcopy, and Graphic Arts III, 1998, vol. 3300, pp. 353-361.
- [2] G. Y. Lin and J. P. Allebach, "Generating stochastic dispersed and periodic clustered textures using a composite hybrid screen," IEEE Transactions on Image Processing, vol. 15, no. 12, pp. 3746-3758, Dec 2006.
- [3] P. Li and J. P. Allebach, "Tone-dependent error diffusion," IEEE Trans. Image Process., vol. 13, no. 2, pp. 201-215, Feb. 2004.
- [4] T. N. Pappas, J. P. Allebach, and D. L. Neuhoff, "Model-based digital halftoning," IEEE Signal Process. Mag., vol. 20, no. 4, pp. 14-27, Jul. 2003.
- [5] C. H. Lee and J. P. Allebach, "The hybrid screen improving the breed," IEEE Trans. Image Process., vol. 19, no. 2, pp. 435-450, Feb. 2010.
- [6] C. Hains, S.-G. Wang, and K. Knox, "Digital color halftones," in Digital Color Imaging Handbook, G. Sharma, Ed. New York: CRC, 2003, pp. 411-416.
- [7] F. A. Baqai and J. P. Allebach, "Computer-aided design of clustered-dot color screens based on a human visual system model," Proceedings of the IEEE, vol. 90, no. 1, pp. 104-122, Jan 2002.
- [8] T. M. Holladay, "An optimum algorithm for halftone generation for displays and hard copies," in Proc. Society Information Display, 1980, vol. 21, pp. 185-192.
- [9] G.-Y. Lin and J. P. Allebach, "Multilevel screen design using direct binary search," J. Opt. Soc. Amer. A, vol. 19, no. 10, pp. 1969-1982, Oct. 2002.
- [10] D. Kacker, T. Camis, and J. P. Allebach, "Electrophotographic process embedded in direct binary search," IEEE Trans. Image Process., vol. 11, no. 3, pp. 243-257, Mar. 2002.

Author Biography

Wan-Eih Huang received her BS in engineering and systems science and MS in electrical engineering from the National Tsing Hua University, Hsinchu, Taiwan, in 2008 and 2010, respectively. After that, she worked at Mstar Semiconductor, Inc., Hsinchu, Taiwan, as a principal engineer in the Digital Display Division.

Currently, she is a Ph.D. student in Purdue University, West Lafayette, IN, where she has been since 2016. Her research interests include image rendering and image quality.

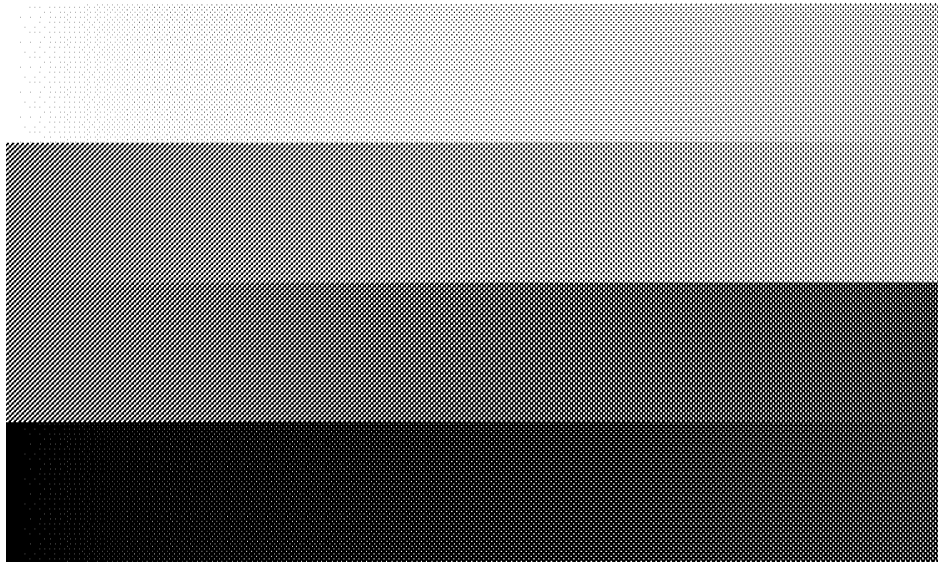


Figure 9: 1.88 in \times 1.12 in halftoned image generated by a 20×24 supercell hybrid screen with square core shape, 4-levels, and unequal spatial resolution (600 dpi \times 400 dpi).

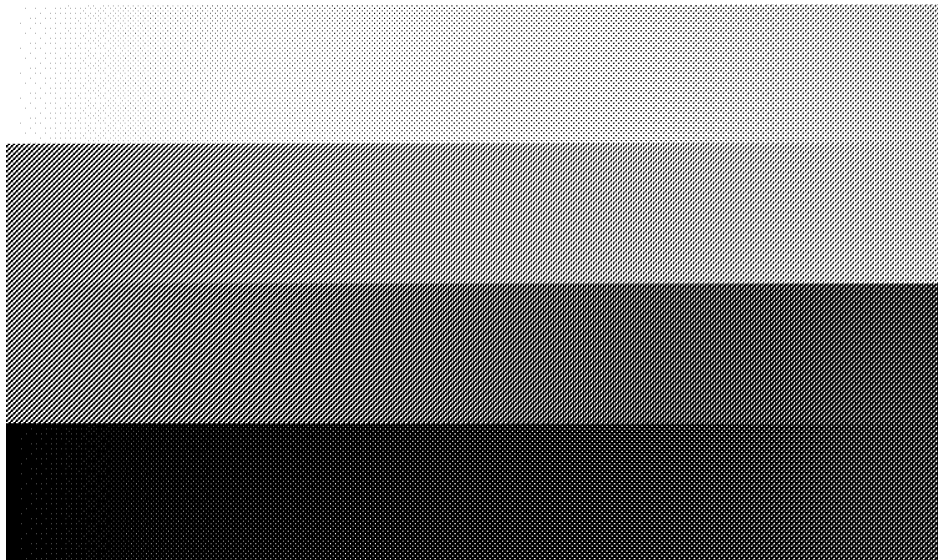


Figure 10: 1.88 in \times 1.12 in halftoned image generated by a 20×24 supercell hybrid screen with S core shape, 4-levels, and unequal spatial resolution (600 dpi \times 400 dpi).